Available online at www.sciencedirect.com
ScienceDirect
Journal of Power Sources 162 (2006) 1373–1378
JOURNAL OF POWER SOURCES
www.elsevier.com/locate/jpowsour

Short communication

The electrochemistry of nanostructured In_2O_3 with lithium

Yongning Zhou, Hua Zhang, Mingzhe Xue, Changliang Wu, Xiaojing Wu, Zhengwen Fu *

Department of Chemistry & Laser Chemistry Institute, Department of Material and Science, Shanghai Key Laboratory of Molecular Catalysts and Innovative Materials Fudan University, Shanghai 200433, PR China

Received 1 August 2006; received in revised form 28 August 2006; accepted 30 August 2006
Available online 9 October 2006

Abstract

The thin films of nanostructured In_2O_3 have been prepared by reactive pulsed laser deposition (PLD) method in oxygen ambient. The electrochemical properties have been investigated by charge/discharge measurement and cyclic voltammograms. A large reversible capacity of nanostructured In_2O_3 thin films was found to be 883 mAh g^{-1}, corresponding to 8.9 Li per In_2O_3. A new couple of reduction and oxidation peaks at 1.0 and 1.9 V were observed from CV curves for the first time. The electrochemical reaction properties of In_2O_3 with lithium were examined by X-ray diffraction (XRD), high resolution transmission electron microscopy (HRTEM) and selected area electron diffraction (SAED) measurements. Both alloying/dealloying processes and oxidation/reduction processes of In were revealed during the lithium electrochemical reaction of In_2O_3 thin film electrode instead of the classical alloying reaction between In_2O_3 and lithium.

Keywords: Thin film; In_2O_3; Lithium batteries; Pulsed laser deposition

1. Introduction

The development and study of new electrode materials and their reaction mechanisms with lithium for rechargeable lithium batteries has become a major topic in the area of the energy storage. In recent years, many studies on transition metal oxides, nitrides and fluorides as the electrode materials of lithium batteries have been made [1–6]. In these studies, the highly reversible electrochemical reactivity of 3d metal oxides with Li at room temperature has drawn much attention in this field. New opportunities seem to be opened for exploring advanced electrode materials and extending concepts in the energy storage region. Accordingly, the legitimate question remains whether this conclusion could be applied to other cases, for instance, whether the reversible formation and decomposition of Li_2O could be driven by indium metal in III_A-group of element table.

Thin films fabrication and characterization of indium trioxide thin films should be paid much attention for its application. There are many deposition techniques currently in use, for example, spray pyrolysis method [7], direct current sputtering [8], metallorganic laser photolysis [9], the sol–gel method [10], pulsed laser deposition (PLD) [11] and so on. Among them, PLD is a useful one for the fabrication of thin films of oxides, especially for nanostructured thin films. However, there is no report on the indium trioxide films fabricated by PLD as storage lithium material.

As far as we know, only Li et al. reported on the electrochemical performance of In_2O_3 electrode prepared by coating slurries of In_2O_3 powder (87% by weight), carbon black (8.7% by weight) and polyvinylidene fluoride (PVDF) (4.3% by weight) dissolved in cyclopentanone on a copper foil substrate [12]. They got the result that reversible reaction of In_2O_3 with Li may be related to the classical alloying process, which is similar to the report of SnO_2 by Coutney and Dahn [13]. However, the electrochemical reaction mechanism of In_2O_3 with Li is still further investigated.

In this paper, we have studied the electrochemical properties of indium trioxide thin films fabricated by pulsed laser deposition, which exhibit an excellent specific capacity and good cycling performance. The structure, composition and morphology of thin films are characterized by X-ray diffraction (XRD), high resolution transmission electron microscopy (HRTEM) and selected area electron diffraction (SAED) measurement. A new electrochemical reaction mechanism of nanostructured In_2O_3

* Corresponding author. Tel.: +86 21 6564 2522; fax: +86 21 6510 2777.
E-mail address: zhengwen@sh163.net (Z. Fu).

0378-7753/$ – see front matter © 2006 Elsevier B.V. All rights reserved.
doi:10.1016/j.jpowsour.2006.08.031

thin film with lithium was found for clarifying the intrinsic properties of In_2O_3 electrode.

2. Experimental

Indium trioxide thin films were fabricated by pulsed laser deposition. The experimental set-up used for PLD has been described elsewhere [14]. A 355 nm laser beam provided by the third harmonic frequency of a Q-switched Nd:yttrium aluminum garnet (YAG) laser (Quanta-Ray GCR-150) was focused on the rotatable target with an angle of 45° to the surface normal. The repetition rate was 10 Hz with a pulse width of 5 ns and the laser fluence was about 2 J cm^{-2}. The deposition chamber was evacuated to a base pressure of about 0.01 Pa and then pure O_2 gas (99.9%) was introduced into the chamber and a pressure of 5 Pa was controlled by a needle valve during deposition. The thin films were deposited on stainless steel substrates, which were kept at 200 °C. Pure In_2O_3 powder (99.999%) was pressed to form a 1.3 cm diameter plate, which was used as targets. The target–substrate distance was 3 cm. The thickness of the as-deposited thin film was measured by a profilometer (Tencor Alpha-Step 200) and was about 180 nm for the deposition time of 20 min. Weight of thin film was directly obtained by subtracting the original substrate weight from total weight of the substrate and deposited thin film onto its surface, which were examined by electrobalance (BP 211D, Sartorius) and was about 0.14 mg with the area of 1.0 cm^2.

A simple three-electrode system was employed in the electrochemical experiments; the as-deposited thin film was served as the working electrode and two sheets of high purity metallic lithium were used as both reference and counter electrodes, respectively. The electrolyte consisted of 1 M $LiPF_6$ in a non-aqueous solution of ethylene carbonate (EC) and dimethyl carbonate (DMC) with a volume ratio of 1:1 (Merck). The cells were assembled in a dry glove box filled with argon. Galvanostatic cycling measurements were carried out with a Land CT2001A battery test system. The cells were cycled between 0.01 and 3.5 V versus Li^+/Li. at a current density of 10 μA cm^{-2}. The cyclic voltammogram (CV) tests were performed with a scanning rate of 0.2 mV s^{-1} between 0.01 and 3.5 V on a CHI660A electrochemical working station (CHI Instruments, TN).

X-ray diffraction patterns and the morphology of the thin film electrodes were recorded by a Bruker D8 advance diffractometer equipped with Cu Kα (λ = 1.5406 Å) and scanning electron microscopy (SEM) (Philips XL30 FEG), respectively. Transmission electron microscopy (TEM) and selected area electron diffraction measurements were carried out by a CM200-FEG TEM at 160 kV accelerating voltage.

The ex situ XRD, TEM and SAED measurements were collected on the lithiated and delithiated In_2O_3 thin film electrodes during the initial discharge and charge process. The model cells were dismantled in an Ar-filled glove box and the electrodes were rinsed in anhydrous, dimethyl carbonate to eliminate residual salts. To avoid exposure to oxygen or water, the thin films or copper grids were rapidly transferred into the chambers for cleanliness.

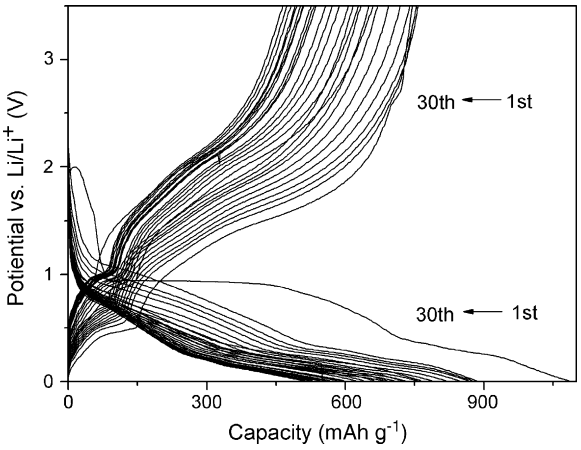

Fig. 1. Voltages composition profiles for the as-deposited In_2O_3 thin film/$LiPF_6$/Li cells. The specific capacity was based on weight of complete thin film. The cells were cycled between 0.01 and 3.5 V vs. Li/Li^+ at a current density of 10 μA cm^{-2}.

3. Result and discussion

The Li storage capacities and cycle performance of In_2O_3 film were investigated by discharge/charge measurements. Fig. 1 shows the discharge and charge curves of Li/In_2O_3 cells cycled between 0.01 and 3.5 V at a constant current density of 10 μA cm^{-2}. The initial open-circuit voltage potential (OCV) of the cell is 2.0 V and two smooth voltage plateaus appear around 1.0 and 0.4 V in the initial discharging process, respectively. Although the stainless steel substrate can react with lithium at lower potentials, the capacity of the stainless steel substrate is less two orders of magnitude than that of In_2O_3 thin film and can be ignored. The discharge plateaus in the galvanostatic curve can be attributed to the electrochemical behavior of the as-deposited film electrode. The capacity of the first discharge is found to be 1083 mAh g^{-1}. This corresponds to 10.8 Li per In_2O_3. The second discharge/charge processes of the cell yield a reversible discharge capacity of 883 mAh g^{-1}, corresponding to 8.9 Li per In_2O_3. It should be noticed that these values are more than the theoretical capacity of Li_3In with 6 Li per In_2O_3 (578 mAh g^{-1}). The plateaus of subsequent charging processes remove towards higher voltage little by little, while the discharge plateaus are ambiguous in the second and subsequent cycles. This may be due to the increase of considerable polarization with further cycles. The capacity fade of the first cycle is about 18.5%, but the fade of 1.7% per cycle after 30 charge/discharge cycles, indicating a highly active In_2O_3 nanostructured thin film with high specific capacities and good coulombic efficiency.

Fig. 2(a) shows the first three cyclic voltammograms for as-deposited thin film electrode of In_2O_3 between 0.01 and 3.50 V measured at a scan rate of 0.2 mV s^{-1}. In the first discharging process, a large peak appears at 1.0 V and the other main two peaks appear at 0.4 and 0.1 V. Compared with the cyclic voltammograms curves of pure metal In (Fig. 2(b)), the latter two peaks can be attributed to the formation of the alloy between In and Li. But the large peak at 1.0 V does not appear in curves of pure indium. It can be attributed to the decomposition of In_2O_3 and the reaction products supplies metal indium for the alloy

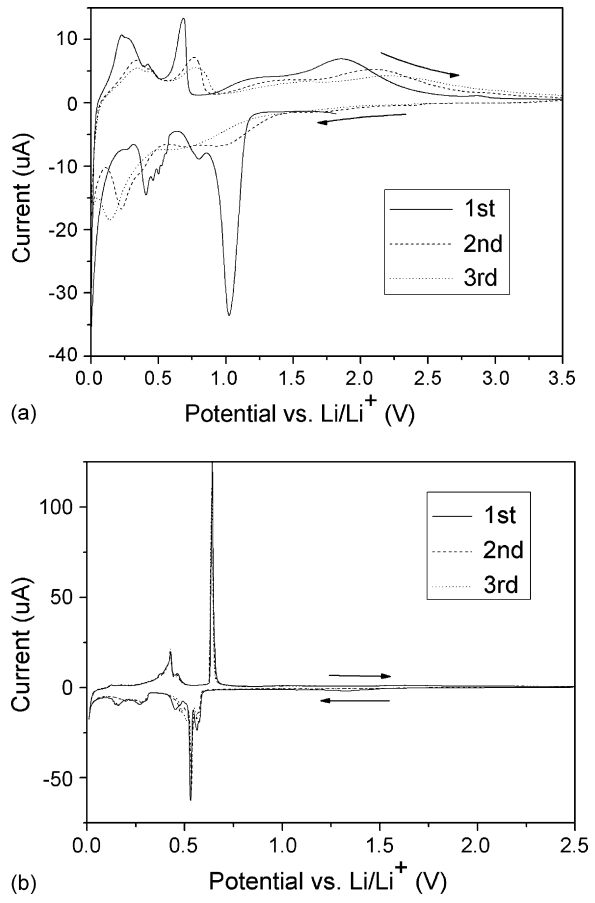

Fig. 2. The first three cyclic voltammograms for the as-deposited In_2O_3 thin film (a) and pure indium thin film (b).

formation with lithium at the potential region less than 1.0 V. In the first charge process of Li/In_2O_3 cell, there are two peaks at 0.3 and 0.7 V same as the charging curves of pure indium, which can correspond to the decomposition of LiIn alloy. Interestingly, we found another oxidation peak at 1.9 V. This may be due to the formation of In_2O_3. In the second cycle, all these peaks are slightly shifted, implying the change of its structure or composition. The reduction peak at 1.0 V fades quickly, indicating large irreversibility of this reaction. But other peaks fade a little. This is in good agreement with the galvanostatic curves.

The XRD patterns of as-deposited, discharged and charged films are shown in Fig. 3. In as-deposited film, the diffraction peaks at $2\theta = 30.5^\circ$ and 35.4° are attributed to cubic structure of In_2O_3 with $Ia3$ space group. Other two diffraction peaks which exist in all three samples at $2\theta = 43.7^\circ$ and 50.8° are attributed to the stainless steel substrate. It can be deduced that the as-deposited films consist of In_2O_3. In the patterns of discharged

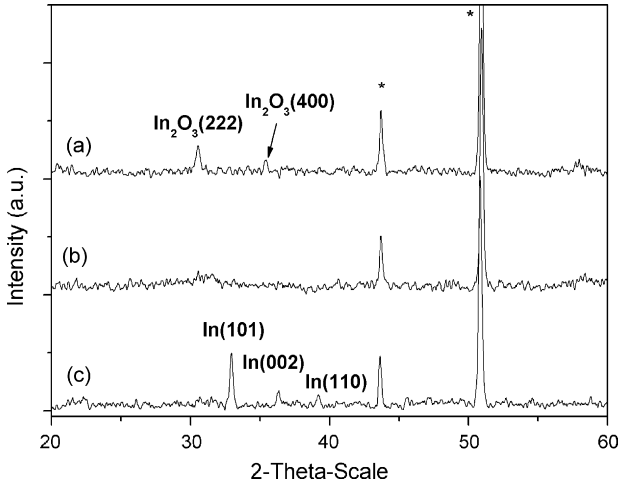

Fig. 3. XRD patterns of the thin films: (a) as-deposited; (b) discharging to 0.01 V; (c) charging to 3.5 V.

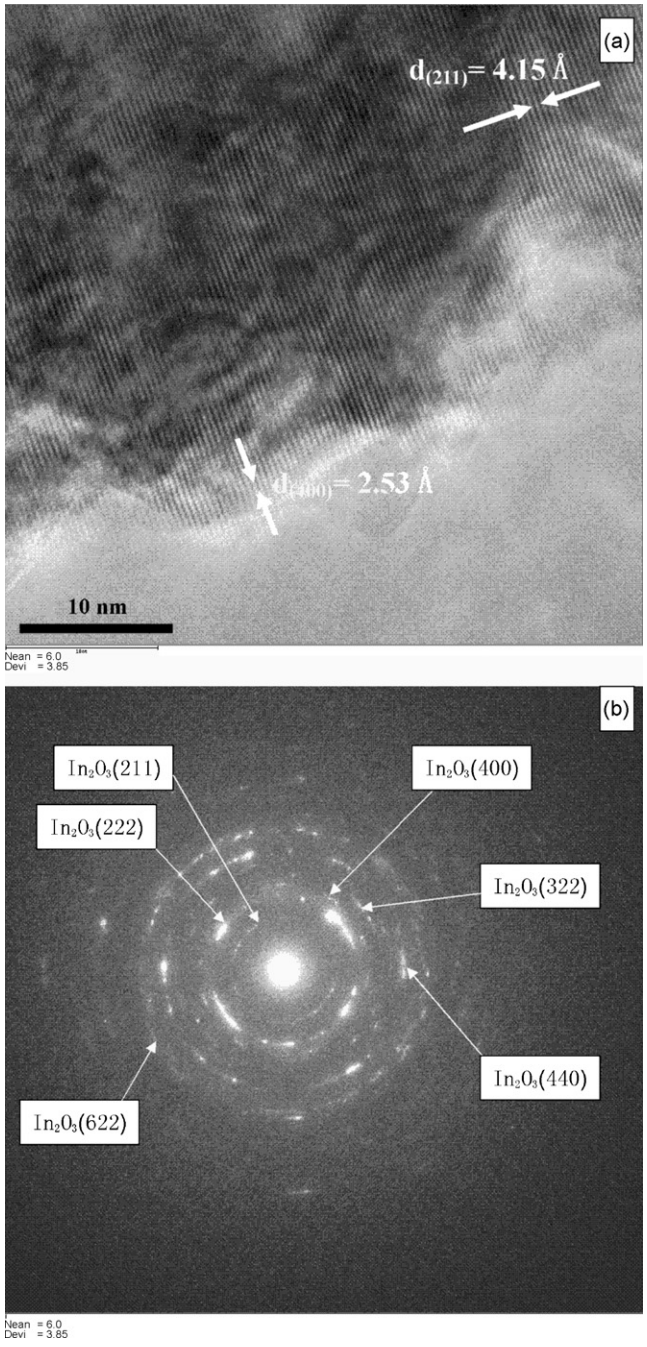

Fig. 4. The ex situ high resolution TEM image (a) and SAED patterns (b) of the as-deposited In_2O_3 thin film fabricated by PLD.

Table 1
d-Spacings derived from SAED analysis of the as-deposited and the first discharging to 0.01 V and the first charging to 3.5 V of In_2O_3 thin film electrode

	In_2O_3 (*Ia*3)		
As-deposited			
4.153	4.131 (2 1 1)		
2.936	2.921 (2 2 2)		
2.524	2.529 (4 0 0)		
2.178	2.157 (3 3 2)		
1.809	1.789 (4 4 0)		
1.517	1.525 (6 2 2)		
$a = 10.16 \pm 0.05$	$a = 10.12$		
	$InLi_2$ (*Cmcm*)		
First discharging to 0.01 V			
2.729	2.734 (1 3 0)		
2.348	2.368 (1 3 1)		
1.668	1.679 (2 0 2)		
1.372	1.372 (3 3 1)		
1.174	1.199 (1 5 1)		
$a = 4.72 \pm 0.03$	$a = 4.76$		
$b = 10.00 \pm 0.04$	$b = 10.02$		
$c = 4.75 \pm 0.02$	$c = 4.74$		
	In_2O_3 (*Ia*3)		In (*I*4/*mmm*)
First charging to 3.5 V			
2.932	2.921 (2 2 2)	2.493	2.473 (0 0 2)
2.043	2.066 (4 2 2)	2.282	2.298 (4 2 0)
1.841	1.848 (1 2 5)	1.489	1.470 (1 0 3)
$a = 10.08 \pm 0.05$	$a = 10.12$	$a = 3.24 \pm 0.04$	$a = 3.25$
		$c = 4.98 \pm 0.02$	$c = 4.95$

JCPDS standards for Ln_2O_3, $InLi_2$ and In shown for reference.

films, there are only two peaks of stainless steel at $2\theta = 33.0^\circ$ and 39.2° and no other peaks can be found in the discharged films. Perhaps the size of reaction products after discharging is less than X-ray coherence length (6 nm), which could not be detected by X-ray diffraction. In charged films, the diffraction peaks at $2\theta = 32.9^\circ$, 36.3° and 39.1° can be assigned to those from metal indium, indicating the existence of metal indium in the charging produce.

In order to further confirm the composition of the discharged and charged products of the films, the ex situ high resolution transmission electron microscopy and selected area electron diffraction measurements were used. Fig. 4(a) shows the high resolution image of the as-deposited film. Two-dimension lattices can be seen clearly in this image. After measuring the *d*-space in two directions, they can be attributed to (2 1 1) and (4 0 0) of In_2O_3, respectively. The SAED pattern in this phase shown in Fig. 4(b) exhibits some rings made up of discrete spots, indicating the nanosized polycrystalline nature of the as-deposited film. All *d*-spacings derived from the SAED spectra could be assigned to In_2O_3 and are shown in Table 1. The space group is *Ia*3. This result is consistent with XRD data.

When the films discharged to 0.01 V, the high resolution image of typical area is shown in Fig. 5(a). SAED pattern in this phase shown in Fig. 5(b) consists of a few rings which can

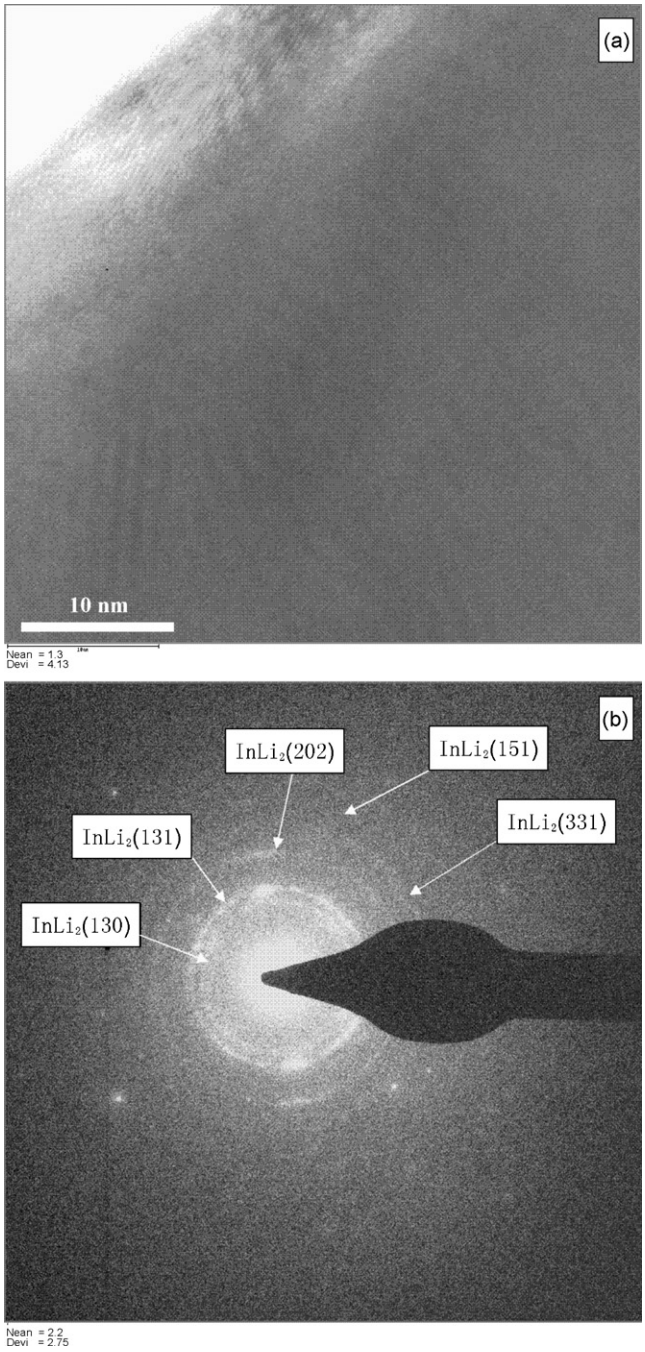

Fig. 5. The ex situ high resolution TEM image (a) and SAED patterns (b) of the In_2O_3 thin film discharging to 0.01 V.

be attributed to $InLi_2$ alloy. The results confirmed the decomposition of In_2O_3 and the formation of $InLi_2$ alloy after the discharging to 0.01 V. However, $InLi_2$ alloy was not observed in XRD pattern shown in Fig. 3(b). This may be due to the fact that the crystal size of electrochemically formed $InLi_2$ is smaller than the X-ray coherence length and is larger than the coherence length of the electron, so it could only be detected by SAED and could not be detected by XRD technique. The HRTEM image after thin film electrode charging to 3.5 V is shown in Fig. 6(a). The crystallites with clear and coherent stripes are observed. The SAED spectrum in this region is shown in Fig. 6(b). The rings

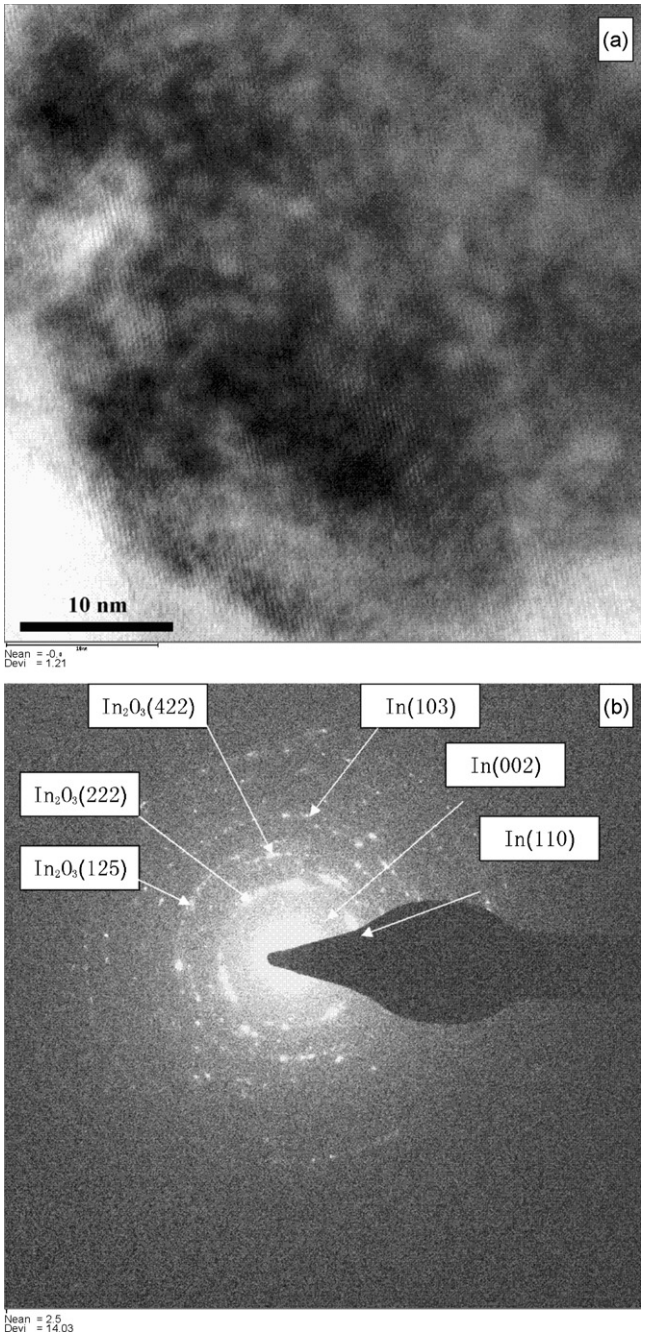

Fig. 6. The ex situ high resolution TEM image (a) and SAED patterns (b) of the In_2O_3 thin film charging to 3.5 V.

consisted of discrete spots were indexed to In and In_2O_3 according to Table 1. This result indicates the produce after charging to 3.5 V consists of In and In_2O_3. The former is observed in XRD pattern shown in Fig. 3(c). The latter could not be detected by XRD techniques, which may be due to the sizes of formed In_2O_3 in the charged film smaller than the X-ray coherence length. The existence of In_2O_3 after charging to 3.5 V provides a direct evidence to conversion reaction of In and Li_2O into In_2O_3.

Based on XRD, TEM and SAED results, the electrochemical reaction mechanism of In_2O_3 with lithium involving the following steps is proposed

$$In_2O_3\,(\text{polycrystalline}) + 10Li^+ + 10e^- \rightarrow 2Li_2In + 3Li_2O \quad (1)$$

$$2Li_2In + 3Li_2O \leftrightarrow In_2O_3\,(\text{nanocrystalline}) + 10Li^+ + 10e^- \quad (2)$$

The irreversible reaction (1) occurs in the first discharging process with the structure transformation of initial polycrystalline In_2O_3 into the nanosized Li_2In and Li_2O. Reaction (2) happens in subsequent cycles and includes two-step reactions. The first step is fully reversible alloying/dealloying reaction of In. The second step involves in the oxidation/reduction reaction of In. The existence of part of metal In in the charged film as shown in Fig. 3, and Fig. 6(b) indicates that In could be not utterly conversed into In_2O_3 and that the second step is a partially reversible reaction. This reaction mechanism can explain the high reversible capacity of 883 mAh g^{-1} (corresponding to 8.9 Li per In_2O_3) in the galvanostatic cycling more than the maximum capacity of Li-alloying with indium (Li_3In, corresponding to 6 Li per In_2O_3). It should be noted that the first discharging capacity is 1083 mAh g^{-1} which corresponds to 10.8 Li per In_2O_3. The capacity is larger than the theoretic capacity deduced from reaction (1). It can be reasonable assumed that a small quantity of Li_XIn ($2 < X < 3$) alloy may exist in the produce after the first discharging.

Combining with the SAED patterns of products in the as-deposited film and the discharging to 0.01 V and charging to 3.5 V, it can be concluded that the new couple of reduction/oxidation peaks at 1.0 and 1.9 V in CV curves can be assigned to the reduction and oxidation of metal indium. Apparently, nanosized metal In could drive the decomposition of Li_2O, this result will change conventional view that reversible reaction of In_2O_3 with Li may be related to the classical alloying process. Although this reaction is not fully reversible, it could increase the reversible capacity remarkably based on the alloying reaction mechanism with lithium and make In_2O_3 a competitive anode material for lithium ion batteries.

4. Conclusion

The PLD method has been used to fabricate nanosized In_2O_3 thin films for the first time. New reaction mechanism was found for the enhancement of reversible capacity and improvement of cycle performance. Galvanostatic cycling showed a reversible capacity of 883 mAh g^{-1}, corresponding to 8.9 Li per In_2O_3. A new couple of reduction and oxidation peaks at 1.0 and 1.9 V in the first cycle were observed from the CV curves of In_2O_3 thin film electrode. Nanostructured thin film of In_2O_3 was found to be one promising candidate of anode materials for rechargeable lithium batteries. Our results demonstrated that the reversible formation and decomposition of Li_2O could be driven by nanosized metal Indium. The results may re-open new opportunities on metal oxides as energy storage materials for rechargeable ion batteries.

Acknowledgement

This work was supported by the National Nature Science Foundation of China (Project No. 20203006).

References

[1] Y. Iodta, US Pat. 547 (1995) 8671.
[2] F. Leroux, G.R. Govrard, W.P. Power, L.F. Nazar, Electrochem. Solid-State Lett. 1 (1998) 255.
[3] P. Poizot, S. Laruelle, S. Grugeon, L. Dupont, J.M. Tarascon, Nature 407 (2000) 496.
[4] M. Nishijima, T. Kagohashi, M. Imanishi, Y. Takeda, O. Yamamoto, S. Kondo, Solid State Ionics 83 (1996) 107.
[5] M.N. Obrovac, R.A. Dunlap, R.J. Sanderson, J.R. Dahn, J. Electrochem. Soc. 148 (2001) A576.
[6] F. Badway, N. Pereira, F. Cosandey, G.G. Amatucci, J. Electrochem. Soc. 150 (2003) A1318.
[7] G. Korotcenkov, V. Brinzari, A. Cerneavschi, M. Ivanov, V. Golovanov, A. Cornet, J. Morante, A. Cabot, J. Arbiol, Thin Solid Films 460 (2004) 315.
[8] P. Malar, Bhasjar Chandra Mohanty, S. Kasiviswanathan, Thin Solid Films 488 (2005) 26.
[9] T. Tsuchiya, A. Watanabe, H. Niino, A. Yabe, I. Yamaguchi, T. Manabe, T. Kumagai, S. Mizuta, Appl. Surf. Sci. 186 (2002) 173.
[10] S.K. Poznyak, A.I. Kulak, Electrochem. Acta 45 (2000) 1595.
[11] F.O. Adurodija, H. Izumi, T. Ishihara, H. Yoshioka, M. Motoyama, Sol. Energy Mater. Sol. Cells 71 (2002) 1.
[12] H. Li, X.J. Huang, L.Q. Chen, Solid State Ionics 123 (1999) 189.
[13] I.A. Coutney, J.R. Dahn, J. Electrochem. Soc. 144 (1997) 2045.
[14] Z.W. Fu, C.L. Li, W.Y. Liu, J. Ma, Y. Wang, Q.Z. Qin, J. Electrochem. Soc. 152 (2005) E50.